Journal of Power Sources 242 (2013) 533–540

Contents lists available at SciVerse ScienceDirect

Journal of Power Sources

journal homepage: www.elsevier.com/locate/jpowsour

Colloidal silica nanoparticle-assisted structural control of cellulose nanofiber paper separators for lithium-ion batteries

Jeong-Hoon Kim [a], Jung-Hwan Kim [a], Eun-Sun Choi [b], Hyung Kyun Yu [b], Jong Hun Kim [b], Qinglin Wu [c], Sang-Jin Chun [d], Sun-Young Lee [d,**], Sang-Young Lee [a,*]

[a] Interdisciplinary School of Green Energy, Ulsan National Institute of Science and Technology (UNIST), Ulsan 689-798, Republic of Korea
[b] Batteries R&D, LG Chem, Yusong-gu, Daejon 305-380, Republic of Korea
[c] School of Renewable Natural Resources, Louisianan State University Agricultural Center, Baton Rouge, LA 70803, USA
[d] Department of Forest Resources Utilization, Korea Forest Research Institute, Seoul 130-712, Republic of Korea

HIGHLIGHTS

- Colloidal SiO_2-assisted structural control of cellulose nanofiber paper separators.
- SiO_2 nanoparticles are introduced as a cellulose nanofiber-disassembling agent.
- Effect of SiO_2 content on separator properties and cell performance is explored.
- The separator (fabricated from SiO_2 = 5 wt.%) imparts the highest ionic conduction.
- As a result, the cell performance of the separator is substantially improved.

GRAPHICAL ABSTRACT

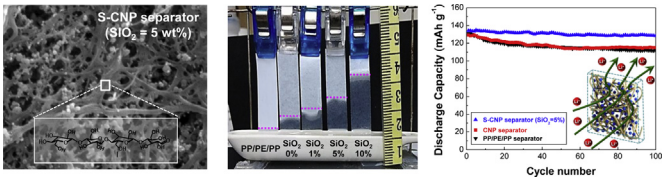

ARTICLE INFO

Article history:
Received 20 March 2013
Received in revised form
22 May 2013
Accepted 26 May 2013
Available online 5 June 2013

Keywords:
Lithium-ion batteries
Separators
Cellulose nanofiber papers
Colloidal silica nanoparticles
Non-conductive spacer particles
Porous structure

ABSTRACT

Porous structure-tuned cellulose nanofiber paper separators (designated as S-CNP separators) are demonstrated as a promising alternative to commercial polyolefin separators for use in lithium-ion batteries. A new architectural strategy based on colloidal silica (SiO_2) nanoparticle-assisted structural control is presented to overcome the difficulty in forming controllable porous structure of pure cellulose nanofiber paper separators (designated as CNP separators) from densely-packed cellulose nanofibers (CNFs). The new S-CNP separators proposed herein incorporate SiO_2 nanoparticles as a CNF-disassembling agent (i.e., as non-conductive spacer particles). This structural uniqueness allows loose packing of CNFs, thereby facilitating the evolution of more porous structure. The unusual porous structure of S-CNP separators can be fine-tuned by varying SiO_2 contents in the CNF suspension. Notably, the S-CNP separator (fabricated with 5 wt.% SiO_2 content) exhibits the highest ionic conduction due to the well-balanced combination of nanoporous structure and separator thickness, thus contributing to excellent cell performance. This study underlines that the colloidal SiO_2 nanoparticle-directed structural tuning of CNPs offers a promising route for the fabrication of advanced paper separators with optimized attributes and functionality.

1. Introduction

Lithium-ion batteries have garnered an increasing attention as a promising power source for rapidly growing application fields such

* Corresponding author. Tel.: +82 52 217 2948.
** Corresponding author. Tel.: +82 2 961 2724.
E-mail addresses: nararawood@forest.go.kr (S.-Y. Lee), syleek@unist.ac.kr (S.-Y. Lee).

0378-7753/$ – see front matter © 2013 Elsevier B.V. All rights reserved.
http://dx.doi.org/10.1016/j.jpowsour.2013.05.142

as smart electronic devices, (hybrid and plug-in) electric vehicles, and grid energy storage systems [1–6]. This strong academic and industrial demand continues to stimulate the development of high-energy density and high-power density cells. However, the effort often confronts some formidable challenges related to safety failure and performance limitation of cells [7–12].

Among various safety issues of the cells, internal short-circuits are known to be one of the most critical threats that are difficult to avoid. A separator (membrane) in the cell is considered a key component to prevent the failures, because its primary function is to maintain electrical isolation between cathode and anode [13–25]. Another major role of a separator is to allow ionic transport via its liquid electrolyte-filled pores. Ionic conductivity of a separator, which strongly depends on its porous structure and polarity, affects ohmic polarization (i.e., IR drop) of a cell. Notably, this influence on cell polarization becomes more pronounced at high current density conditions needed for high-power applications.

In current commercial lithium-ion batteries, most widely adopted separators are manufactured from polyolefins, predominantly polyethylene (PE) and polypropylene (PP) [13–15]. These polyolefin separators have well-tailored physical and electrochemical properties in terms of practical application to cells. However, their poor thermal stability, low porosity, and insufficient electrolyte wettability often raise serious concerns about ionic transport (affecting cell performance) and electrical isolation (related to cell safety) between electrodes.

Meanwhile, as a new approach to overcome these stringent drawbacks of conventional polyolefin separators, our group has recently developed eco-friendly cellulose nanofiber paper-derived separators (referred to as "CNP separators") [26] as a promising alternative to synthetic polymer-based separators. The CNP separators are featured with an electrolyte-philic, nanoscale labyrinth structure established between closely piled cellulose nanofibers (CNFs), in contrast to typical papers comprising macro/microscopic cellulose fibers. Owing to the unusual thermal stability and polarity of the CNFs, the CNP separators provide substantial improvement in the thermal shrinkage and electrolyte wettability, as compared to commercial tri-layer (polypropylene (PP)/polyethylene (PE)/polypropylene (PP)) separators. Despite these advantageous characteristics, however, the CNP separators suffer from some limitations in providing high-porous structure. This drawback of the CNP separators may stagger ionic transport via the liquid electrolyte-filled CNP separator. This structural shortcoming may arise from the dense packing [27–32] of CNFs composed of close-packed polysaccharide chains with β-(1 → 4)-D-glucopyranose repeat units (i.e., cellulobiose unit).

Herein, in an effort to resolve the aforementioned challenge of the CNP separators, a new architectural strategy based on colloidal silica (SiO_2) nanoparticle-assisted control of porous structure is proposed. The SiO_2 nanoparticles are introduced as a CNF-disassembling agent (i.e., as non-conductive spacer particles). More specifically, they are dispersed between the CNFs and allow loose packing of CNFs, thereby facilitating the evolution of more porous structure. This demonstrates that the nanoscale labyrinth structure (i.e., nanoporous structure) of CNP separators can be finely-tuned by varying SiO_2 contents in the CNF suspension.

Membrane characteristics of SiO_2-incorporated CNP separators (referred to as "S-CNP separators"), including porous structure, electrolyte wettability, and ionic conductivity, are examined as a function of SiO_2 content in the CNF suspension. Based on this understanding, effects of the S-CNP separators on cell performance (in particular, under high-current density conditions) are scrutinized and discussed with an in-depth consideration of their structural uniqueness. Meanwhile, as a control sample, a commercial tri-layer PP/PE/PP separator, one of the most widely used separators in mid to large-sized cells for (hybrid) electric vehicles and grid energy storage systems, is used.

2. Experimental

2.1. Fabrication of SiO_2-incorporated cellulose nanofiber paper separators ("S-CNP separators")

The CNF suspension for fabricating S-CNP separators was obtained by homogenizing cellulose powders (particle size ~ 45 μm, KC Flock, Nippon Paper Chemicals) in IPA/water (=95/5 v/v) mixture solvent. The detailed procedure for preparing the CNF suspension has been described in our previous publication [26]. Colloidal SiO_2 nanoparticles (average particle size ~ 100 nm, Nissan) dispersed in water were then added into the CNF suspension, wherein the SiO_2 content was controlled at 0, 1, 5, and 10 wt.% relative to the CNF weights. After vigorous mixing, the CNF/SiO_2 mixture suspension was poured onto a filter paper positioned onto a Porcelain Buchner funnel and then subjected to vacuum filtration, yielding a wet CNF/SiO_2 paper. The wet paper was inserted between two filter papers and subsequently dried under a pressure of 1 MPa in a hot-oven at 80 °C for 48 h, resulting in the formation of a SiO_2-incorporated CNP separator (i.e., S-CNP separator). The final thickness of the S-CNP separator increased slightly as the incorporated SiO_2 content was increased. A commercial tri-layer (PP/PE/PP) separator (thickness = 20 μm, Celgard) was chosen as a control sample.

2.2. Membrane properties and electrochemical performance of SiO_2-incorporated cellulose nanofiber paper separators ("S-CNP separators")

The porous structure of S-CNP separators was observed using a field emission scanning electron microscope (FE-SEM, Hitachi). The air permeability of separators was evaluated with a Gurley densometer (4110N, Gurley) by measuring the time necessary for air to pass through a determined volume under a given pressure, where a low Gurley value (sec 100 cc^{-1}) represents high air permeability [13–20]. The porosity (ϕ_p) of S-CNP separators was estimated by observing their density difference before and after solvent uptake (Galwick™ with density = 1.83 g cc^{-1} as solvent) [33–36]. The thermal shrinkage of S-CNP separators was determined by measuring their area-based dimensional change (=ΔA) after heat treatment at 150 °C for 0.5 h [17–19]. As a liquid electrolyte to infiltrate into pores of S-CNP separators, 1 M $LiPF_6$ in ethylene carbonate (EC)/diethyl carbonate (DEC) (=1/1 v/v, Soulbrain) was employed. The electrolyte wettability of S-CNP separators was elucidated by monitoring turbidity change of separator surface after dropping the liquid electrolyte onto separators and also was quantitatively estimated by measuring electrolyte immersion-height. The electrochemical stability window of S-CNP separators was investigated using a linear sweep voltammetry experiment performed on a working electrode of stainless-steel and a counter and reference electrode of lithium-metal at a scan rate of 1.0 mV s^{-1}. The ion conductivity of S-CNP separators was obtained by an AC impedance analysis (VSP classic, Bio-Logic) over a frequency range of 10^{-2}–10^{6} Hz. A unit cell (2032-type coin) was assembled by sandwiching a separator between a natural graphite anode (natural graphite/CMC/SBR = 97.5/1.0/1.5 w/w/w) and a $LiNi_{1/3}Mn_{1/3}Co_{1/3}O_2$ cathode ($LiNi_{1/3}Mn_{1/3}Co_{1/3}O_2$/carbon black/PVdF = 95/2/3 w/w/w), and then activated by filling it with the liquid electrolyte. All assembly of cells was carried out in an argon-filled glove box. The discharge capacities, discharge C-rate capability, and cycling performance of cells were evaluated using a cycle tester (PNE Solution). The discharge current densities were varied

from 0.2 (=0.224 mA cm^{-2}) to 3.0 C at a constant charge current density of 0.2 C under a voltage range between 3.0 and 4.2 V. For the measurement of cycling performance, the cells were cycled at a constant charge/discharge current density of 1.0 C/1.0 C.

3. Results and discussion

3.1. Effect of SiO_2 content on membrane properties of S-CNP separators

Our previous study [26] reported that the CNFs obtained from high-pressure homogenization are characterized with nanometer-scale diameters, length up to several micrometers and dense crystalline packing (Fig. 1(a)). These structural features of the CNFs play a key role in providing substantial improvement in mechanical and thermal properties, and also in realizing the unusual nanoporous structure (i.e., labyrinth structure) of the CNP separator (i.e., SiO_2 = 0 wt.%). Fig. 1(b) shows that nano-sized pores are formed between the highly interconnected CNFs and are distributed over a wide area of the CNP separator [26]. In the fabrication of the CNP separator, the CNFs readily collapse by capillary action [30,37] during evaporation of solvent mixture (=water/IPA) and then the deformed state of CNFs is fixed by strong hydrogen bonds of polysaccharide chains.

Membrane properties of the S-CNP separators were examined as a function of SiO_2 content and discussed in terms of the CNF structure. As the SiO_2 content in the CNF suspension is increased from 1 to 10 wt.%, larger numbers of SiO_2 particles are dispersed between the CNF fibers in the S-CNP separators (Fig. 1(c)–(e)). A notable finding is that the porous structure of S-CNP separators is strongly dependent on the SiO_2 content in the CNF suspension. At a low SiO_2 content (for example, SiO_2 = 1 wt.%), the overall porous structure (Fig. 1(c)) appears to be negligibly different from that (Fig. 1(b)) of the CNP separator. On the other hand, with increasing SiO_2 content, the porous structure of the S-CNP separators is more developed. This indicates that the SiO_2 nanoparticles are dispersed between the CNFs and then act as non-conductive spacer particles, thereby impeding dense packing of CNFs during the solvent evaporation. As a result, the more developed porous structure is obtained at the resulting S-CNP separators. Unfortunately, the dispersion state of SiO_2 nanoparticles in the S-CNP separators is not sufficiently satisfying, which will be further improved in our future studies. Meanwhile, in comparison to these S-CNP separators, the commercial PP/PE/PP separator (herein, its PP outer layer is observed) has a number of slit-like pores in a pocket fashion (Fig. 1(f)), where the pores are formed between uniaxially deformed PP lamellar crystallines [13–15].

This morphological result demonstrates that the incorporation of SiO_2 nanoparticles in the CNF suspension is an effective way to control nanoscale labyrinth structure (i.e., nanoporous structure) of CNP separators. The intriguing behavior of SiO_2 content-directed morphological variation in the S-CNP separators is schematically illustrated in Fig. 2. Here, it should be noted that the nanoporous region of S-CNP separators is filled with liquid electrolytes during

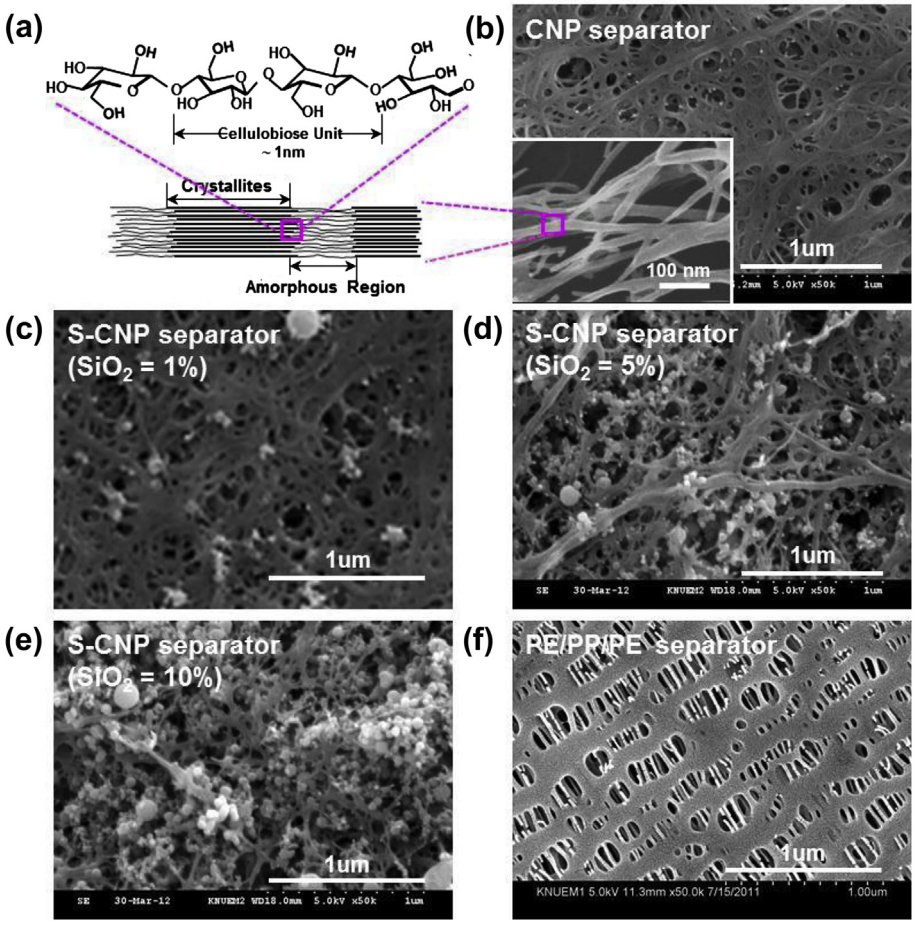

Fig. 1. (a) A schematic representation depicting crystalline–amorphous structure of CNFs that comprise close-packed polysaccharide chains with β-(1 → 4)-D-glucopyranose repeat units. FE-SEM photographs of: (b) CNP separator, where an inset indicates a high-magnification image; (c) S-CNP separator (SiO_2 = 1 wt.%); (d) S-CNP separator (SiO_2 = 5 wt.%); (e) S-CNP separator (SiO_2 = 10 wt.%); (f) PP/PE/PP separator.

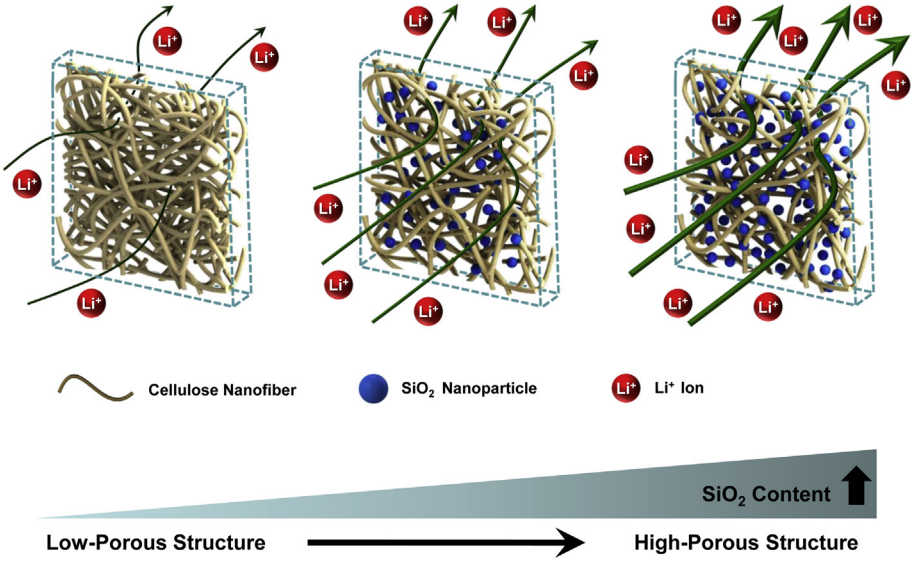

Fig. 2. A schematic illustration demonstrating SiO_2 content-directed morphological variation in the S-CNP separators and its influence on ionic transport of the separators.

cell assembly and thereupon functions as effective ion-conductive channels.

The porous structure of S-CNP separators was quantitatively characterized by measuring their Gurley value (i.e., air permeability) and porosity. Table 1 shows that, as the SiO_2 content in the CNF suspension is increased, the Gurley values of the S-CNP separators tend to decrease. Notably, these Gurley values of the S-CNP separator are lower than that (=500 s 100 cc^{-1}) of the PP/PE/PP separator. It is known that a low Gurley value of a separator represents high air permeability, i.e., a short tortuous path for air transport [13–20]. As another evidence to prove the porous structure of S-CNP separators, the variation in their porosity was examined as a function of SiO_2 content. Table 1 also exhibits that the porosities of the separators are, respectively, 40% for the CNP separator, 48% for the S-CNP separator (SiO_2 = 5 wt.%), and 52% for the S-CNP separator (SiO_2 = 10 wt.%), as compared to that (=41%) of the PP/PE/PP separator. Therefore, the decrease in the Gurley value and also the increase in the porosity of the S-CNP separators verify the formation of a highly-developed porous structure due to the addition of SiO_2 nanoparticles, which is well-consistent with the previous morphological results (Fig. 1).

This intriguing relationship between the porous structure and Gurley value (& porosity) of the S-CNP separators was further confirmed by measuring their ionic conductivity. Table 1 exhibits that the ionic conductivity of S-CNP separators increases from 1.41 to 2.40 mS cm^{-1} with an increase of SiO_2 content (from 0 to 10 wt.%), which is inversely proportional to the change of the Gurley value. Previous studies [13–15] reported that the air permeability (i.e., Gurley value) may be a useful parameter to predict ionic conductivity of separators, where low Gurley value reflects high ionic conductivity.

From these results of ionic conductivity, the MacMullin number [14,26] ($N_M = \sigma_o/\sigma_s$, wherein σ_o = ionic conductivity of liquid electrolyte, σ_s = ionic conductivity of liquid electrolyte-filled separator) of the separators was estimated. The N_M is known to indicate the loss of ionic conductivity due to the presence of a porous substrate (herein, a separator membrane). Table 1 shows that the N_M value of S-CNP separators is drastically decreased at higher SiO_2 contents. For example, the N_M value of the S-CNP separator (SiO_2 content = 5 wt.%) is found to be 2.54, which is lower than that (=10.3) of the PP/PE/PP separator. This underlines that the highly-interconnected nanoporous network channels are successfully developed in the S-CNP separator, owing to the introduction of SiO_2 spacer particles. The strong dependence of ionic transport on the morphological variation of S-CNP separators is also schematically illustrated in Fig. 2.

Meanwhile, considering practical application of separators to lithium-ion batteries, the ionic conductance ($G[S] = (\sigma \times A)/l$, where σ is ionic conductivity [S cm^{-1}], A is sample area, and l is sample thickness) of a separator is a more important factor that exerts a direct influence on cell performance, rather than ionic conductivity (σ) that is normalized by separator thickness [14,38]. For instance, a thick separator is likely to provide long path for ionic migration, yielding low ionic conductance. As a consequence, this may give rise to an increase in ohmic polarization (i.e., IR drop) of cells, leading to the decline in cell performance. Table 1 shows that the thickness of S-CNP separator is larger with increasing SiO_2 content (25 μm at CNP separator → 32 μm at SiO_2 = 5 wt.% → 37 μm at

Table 1
Membrane properties of a commercial tri-layer (PP/PE/PP) separator, CNP separator, and S-CNP separators as a function of SiO_2 content.

SiO_2 content (wt.%)	Thickness [μm]	Gurley value [s 100 cc^{-1} air]	Porosity [%]	Ionic conductivity [mS cm^{-1}, σ_{eff}]	McMullin number[a]	Ionic conductance [S]
0	25	512	40	1.41	5.36	1.13
1	28	340	42	1.92	3.93	1.38
5	32	314	48	2.97	2.54	1.86
10	37	280	52	2.40	3.15	1.31
PP/PE/PP separator	20	500	41	0.73	10.3	0.73

[a] McMullin number (N_M) = σ_o/σ_s. σ_o = ionic conductivity of liquid electrolyte (=7.552 mS cm^{-1}). σ_s = ionic conductivity of liquid electrolyte-filled separator.

SiO_2 = 10 wt.%). This increase in the separator thickness impairs the ionic conductance of separators. Therefore, it can be reasonably speculated that the ionic conductance of S-CNP separators at higher SiO_2 content may be traded-off by highly-developed porous structure (=advantageous effect) and separator thickness (=negative effect). Notably, the optimized value of ionic conductance (=1.86 S) is obtained at SiO_2 content = 5 wt.%, which is also confirmed by the lowest N_M (=2.54). This higher ionic conductance of the S-CNP separator is expected to beneficially influence cell performance, which will be discussed in great detail in the following section.

Polyolefin separators are known to be intrinsically hydrophobic, raising serious concerns about liquid electrolyte wettability [13–15]. More importantly, in mid to large-sized batteries, which have attracted considerable attention in rapidly growing application fields such as (hybrid) electric vehicles and grid storage systems, fast and uniform wetting of liquid electrolytes over an entire separator is strongly demanded. Fig. 3(a) shows that, as compared to the PP/PE/PP separator, the S-CNP separator (SiO_2 = 5 wt.%) as well as CNP separator is quickly wetted with the liquid electrolyte (1 M $LiPF_6$ in EC/DEC = 1/1 v/v), where the electrolyte droplets rapidly spread over a wide area of the separators.

This superior wettability of the S-CNP separators is quantitatively evaluated by measuring their electrolyte immersion-height (Fig. 3(b)). After an elapsed time of 1 h, the S-CNP separators show the greater electrolyte immersion-height than the PP/PE/PP separator. Another intriguing finding is that the electrolyte immersion-height of S-CNP separators is higher with increasing SiO_2 content (~0.6 cm at SiO_2 = 0 wt.% → ~1.2 cm at SiO_2 = 5 wt.% → ~2.1 cm at SiO_2 = 10 wt.%). This may be attributed to the improvement in polarity (i.e., electrolyte-philicity) of S-CNP separators by the addition of hydrophilic SiO_2 nanoparticles [38–41]. This beneficial contribution of the incorporated SiO_2 particles, in combination with the polar CNFs and well-interconnected

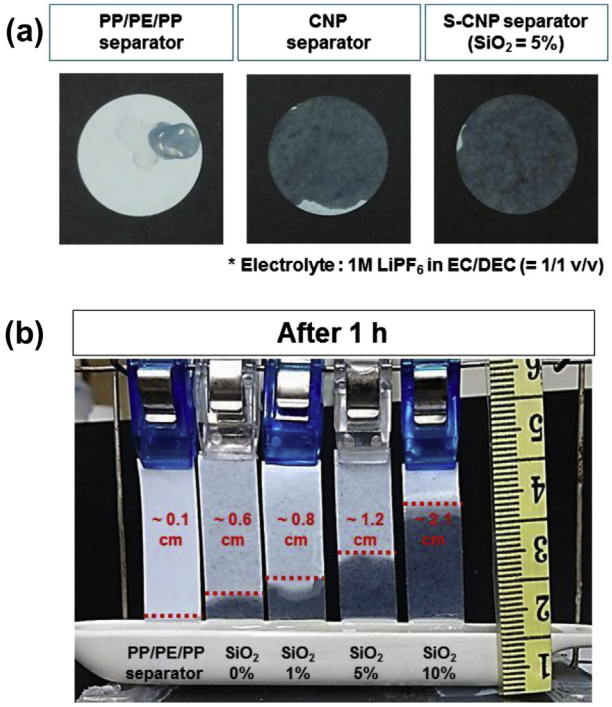

Fig. 3. Comparison of liquid electrolyte wettability between PP/PE/PP separator, CNP separator, and S-CNP separators (SiO_2 = 1, 5, 10 wt.%): (a) photographs showing liquid electrolyte (1 M $LiPF_6$ in EC/DEC = 1/1 v/v) wetting behavior; (b) liquid electrolyte immersion-height.

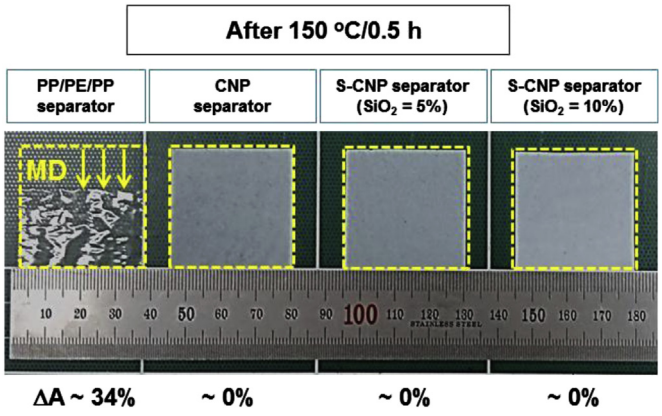

Fig. 4. Thermal shrinkage (=Δ*A*) of PP/PE/PP separator, CNP separator, and S-CNP separators (SiO_2 = 5, 10 wt.%) after exposure to 150 °C for 0.5 h.

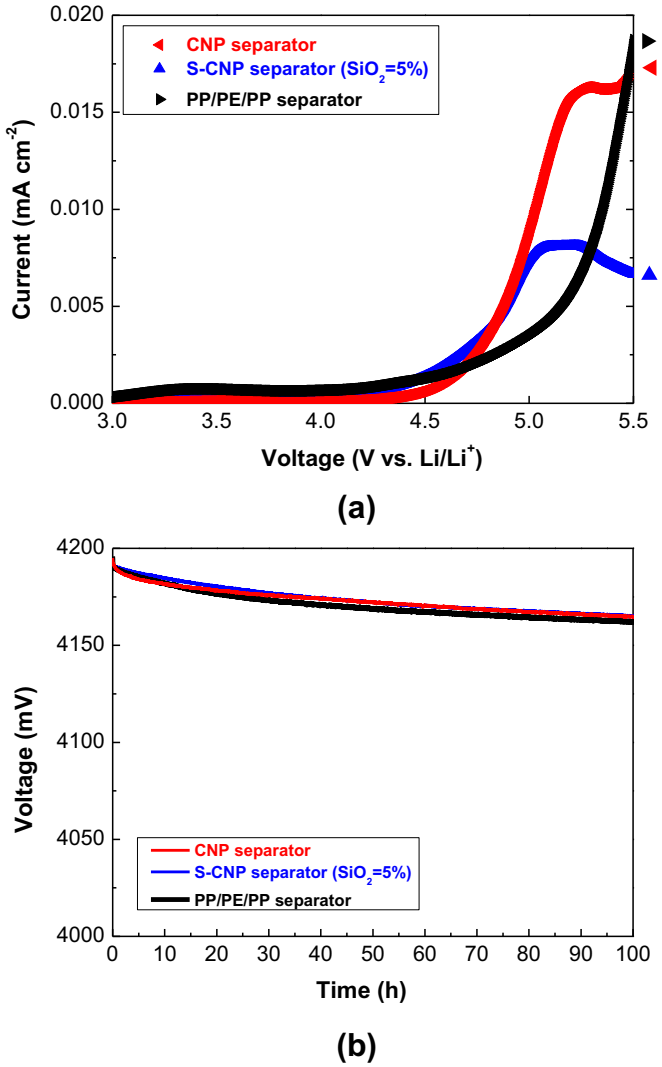

Fig. 5. (a) Linear sweep voltammograms of PP/PE/PP separator, CNP separator, and S-CNP separator (SiO_2 = 5 wt.%) at a voltage scan rate of 1.0 mV s^{-1}. (b) OCV profiles of cells assembled with PP/PE/PP separator or CNP separator or S-CNP separator (SiO_2 = 5 wt.%), wherein the cells are charged to 4.2 V at a constant charge current density of 0.2 C and their voltage drop is measured as a function of elapsed time.

nanoporous network channels, is expected to facilitate capillary intrusion [17–19,26] of liquid electrolyte into pores of S-CNP separators.

Fig. 4 shows a comparison of the thermal shrinkage of the S-CNP separators with that of the PP/PE/PP separator by observing the area-based dimensional change (=Δ*A*), where the separators were exposed to 150 °C for 0.5 h. At this high temperature condition, the PP/PE/PP separator shows the large thermal shrinkage (Δ*A* ~ 34%), as expected. In contrast, the dimensional change of the S-CNP separators appears to be negligible (Δ*A* ~ 0%). Intriguingly, no significant difference in the dimensional change is observed between the S-CNP separators. This remarkably suppressed thermal shrinkage of the S-CNP separators is mainly due to structural and thermal robustness of their components such as CNFs and SiO_2 nanoparticles, along with no involvement of stretching processes during the separator fabrication.

3.2. Characterization of electrochemical performance of cells assembled with S-CNP separators as a function of SiO_2 content

The effects of the S-CNP separators having varied SiO_2 contents on electrochemical performance, including the electrochemical stability window, OCV (Open Circuit Voltage) drop, and cell performance, were investigated and discussed in terms of the abovementioned membrane properties of S-CNP separators.

The electrochemical stability window of the CNP separator and S-CNP separator (SiO_2 content = 5 wt.%) was evaluated by observing linear sweep voltammograms. Fig. 5(a) shows that no appreciable decomposition of any components in the separators takes place below 4.5 V vs. Li/Li^+, which is almost comparable to that of the PP/PE/PP separator. This result demonstrates the good electrochemical stability of the S-CNP separator as well as CNP separator, revealing that they could be as a promising alternative to the PP/PE/PP separator for potential use in high-voltage lithium-ion batteries.

The OCV drop of cells, which provides useful information on self-discharge and also possibly predicts the risk of internal short-circuits between electrodes during cycling, is known to be strongly affected by porous structure of separators [14,17–19]. For instance, a separator with excessively large-sized pores and non-uniform pore size distribution often fails to adequately prevent leakage current between electrodes, resulting in a sharp decline of the OCV. The cells, which had the same cell configuration (i.e., $LiNi_{1/3}Mn_{1/3}Co_{1/3}O_2$ cathode/separator/natural graphite anode) as the one used for cell characterization, were charged to 4.2 V and their voltage drop was monitored as a function of elapsed time. Fig. 5(b)

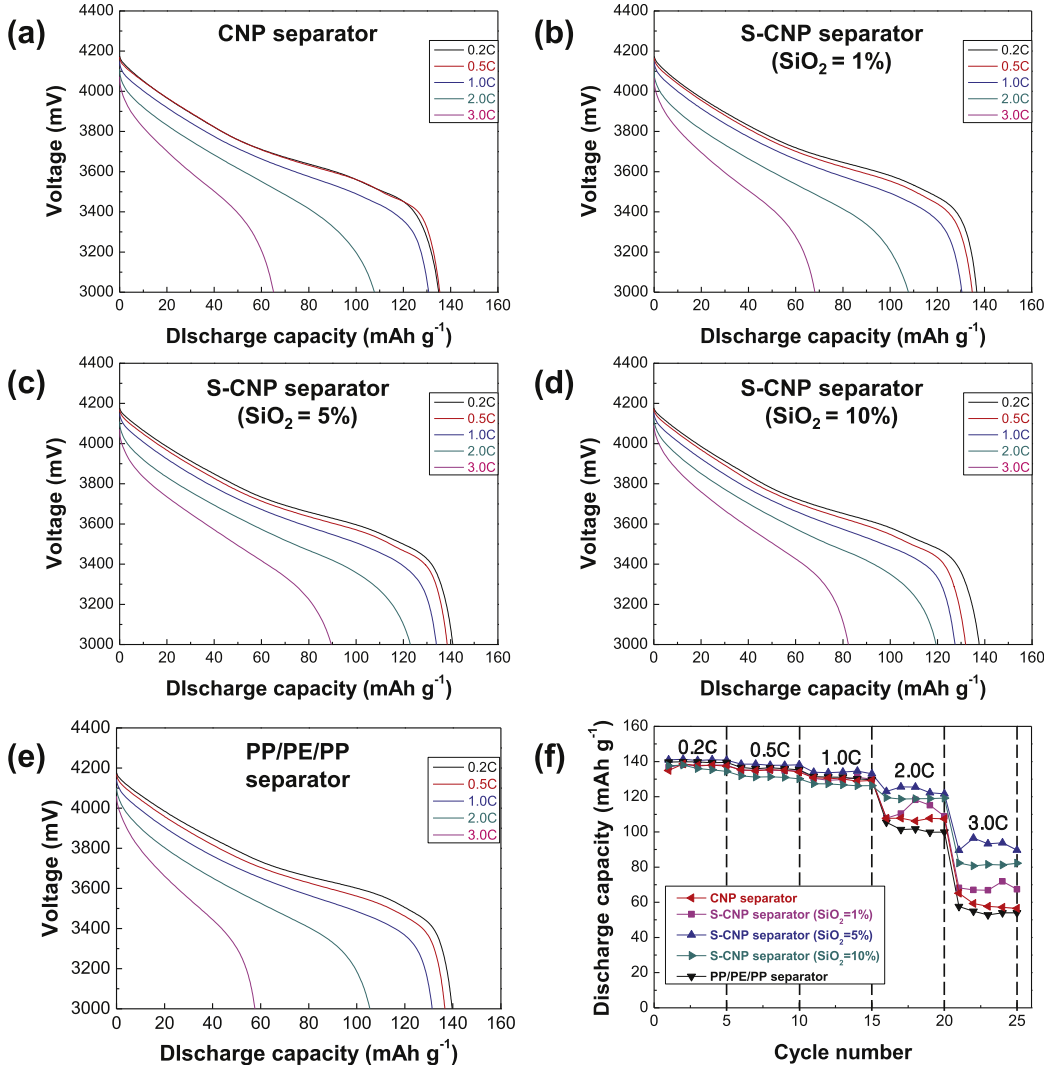

Fig. 6. Discharge profiles of cells assembled with: (a) CNP separator; (b) S-CNP separator (SiO_2 = 1 wt.%); (c) S-CNP separator (SiO_2 = 5 wt.%); (d) S-CNP separator (SiO_2 = 10 wt.%); (e) PP/PE/PP separator. (f) Comparison of discharge C-rate capability between CNP separator, S-CNP separators, and PP/PE/PP separator.

shows that the cells assembled with the CNP separator and S-CNP separators (5 wt.% SiO_2) do not present detectable OCV drop even after an elapsed time of 100 h. Moreover, an inappreciable difference in the OCV profiles was observed between the cellulose paper separators and the PP/PE/PP separator. This excellent OCV behavior of the cellulose paper separators can be explained by considering their unique porous structure. The morphological results (Fig. 1) show that both the CNP separator and S-CNP separator (5 wt.% SiO_2) have the nano-sized pores and narrow pore size distribution, which could be comparable to those of the PP/PE/PP separator. Therefore, it is reasonably expected that the porous structure of the S-CNP separator as well as CNP separator is sufficiently tuned to suppress self-discharge of cells.

The cell performance of S-CNP separators was examined at various charge/discharge conditions as a function of SiO_2 content. Fig. 6 depicts the discharge profiles of cells assembled with S-CNP separators, wherein the cells were charged under a voltage range of 3.0–4.2 V at a constant charge current density of 0.2 C and discharged at various current densities ranging from 0.2 to 3.0 C. For all the separators, the voltage and discharge capacity of cells gradually decrease with an increase of discharge current density. Intriguingly, as the SiO_2 content is increased, the S-CNP separators deliver higher discharge capacities over a wide range of discharge current densities. This gap in the discharge capacities between the different S-CNP separators becomes more pronounced at higher discharge current densities where the influence of ionic conduction of a separator on ohmic polarization of a cell is more important [13–20]. Meanwhile, the S-CNP separators exhibit the better discharge C-rate capability than the commercial PP/PE/PP separator (Fig. 6(e)).

Fig. 6(f) summarizes the discharge capacities of the S-CNP separators as a function of discharge current density (i.e., discharge C-rate). The previous morphological results (Fig. 1 and Table 1) showed that, with increasing SiO_2 content, a more porous structure is developed in the S-CNP separators owing to the beneficial contribution of SiO_2 nanoparticles serving as spacer particles, possibly yielding a shorter tortuous path for ionic transport. As a consequence, the S-CNP separator with larger SiO_2 content can allow facile ionic transport (Table 1), contributing to the excellent discharge C-rate capability. Another notable finding is that, among the S-CNP separators examined herein, the S-CNP separator fabricated with 5 wt.% SiO_2 shows the highest discharge C-rate capability. This can be explained by considering the ionic conductance of the S-CNP separators. Table 1 shows that the S-CNP separator (SiO_2 content = 5 wt.%) presents the highest ionic conductance (=1.86 S) than other S-CNP separators due to the favorable combination of highly-developed porous structure and low separator thickness. Hence, this excellent ionic conductance of the S-CNP separator (SiO_2 content = 5 wt.%) is believed to exert a beneficial influence on mitigating the ohmic polarization loss of cells (Fig. 6(a)–(d)), leading to the improvement of discharge C-rate capability.

The cycling performance of CNP separator and S-CNP separator (SiO_2 content = 5 wt.%) was investigated, where the cells were cycled between 3.0 and 4.2 V at a constant charge/discharge current density (=1.0 C/1.0 C). Fig. 7 shows that the S-CNP separators provide no abnormal or unstable charge/discharge profiles and, moreover, good charge/discharge capacities up to the 100th cycle. The S-CNP separator (Fig. 7(b)) exhibits the better capacity retention during cycling, as compared to the CNP separator (Fig. 7(a)) and PP/PE/PP separator (Fig. 7(c)). The cycling performance of the different separators is summarized and compared in Fig. 7(d). The discharge capacity retention after the 100th cycle is found to be 89.1% for the CNP separator, 95.5% for the S-CNP separator, and 85.3% for the PP/PE/PP separator, respectively. This excellent cycling performance of the S-CNP separator may be ascribed to its highly-developed nanoporous structure (Fig. 1) and strong affinity for liquid electrolyte (Fig. 3), contributing to the high ionic conductivity, fast and uniform electrolyte wetting, and good electrolyte retention during cycling. Meanwhile, there is no doubt that deterioration of cycling performance may be possibly caused by

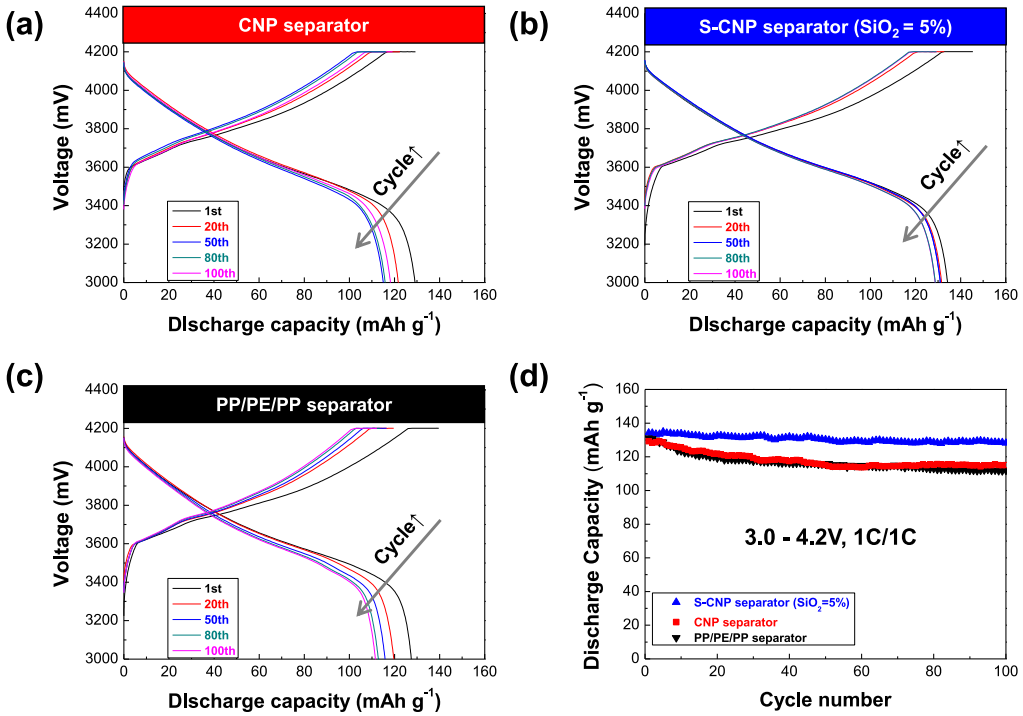

Fig. 7. Charge/discharge profiles (during cycling) of cells assembled with: (a) CNP separator; (b) S-CNP separator (SiO_2 = 5 wt.%); (c) PP/PE/PP separator. (d) Comparison of cycling performance between CNP separator, S-CNP separators, and PP/PE/PP separator.

continued growth of undesired resistive layers formed on electrodes, which would in turn bring serious polarization at electrolyte–electrode interface [42–44] A more detailed elucidation on structural change of electrode surface and cell impedance variation during cycling will be conducted in future studies.

The abovementioned results of electrochemical characterization demonstrate that the incorporation of SiO_2 nanoparticles (acting as spacer particles) into the CNFs is an effective way to fabricate advanced cellulose paper separators with excellent cell performance.

4. Conclusion

The porous structure-tuned cellulose nanofiber paper separators (S-CNP separators) were developed via a facile fabrication strategy based on colloidal SiO_2 nanoparticle-assisted structural control. The SiO_2 nanoparticles were introduced as a CNF-disassembling agent. In comparison to the CNP separator containing no SiO_2 nanoparticles, the S-CNP separators allowed the loose packing of CNFs due to the presence of SiO_2 nanoparticles (serving as non-conductive spacer particles) dispersed between the CNFs, thereby facilitating the evolution of more porous structure. This structural uniqueness of the S-CNP separators, in combination with their high polarity, brought significant improvements in the ionic conductivity and electrolyte wettability. Notably, as the SiO_2 content was increased, the S-CNP separators showed a highly-developed porous structure (i.e., high porosity and low Gurley value) without impairing the OCV drop behavior. As a result, the SiO_2 content-directed morphological variation of S-CNP separators exerted substantial influence on the cell performance. Among the S-CNP separators explored herein, the S-CNP separator (fabricated with 5 wt.% SiO_2) provided the best cell performance. This excellent cell performance of the S-CNP separator (SiO_2 content = 5 wt.%) was attributed to its highest ionic conduction arising from the well-balanced properties between the porous structure and separator thickness. These results underline that the S-CNP separator with well-developed porous structure and optimized membrane properties could be a promising alternative to outperform a commercial PP/PE/PP separator used in mid to large-sized lithium-ion batteries targeting (hybrid) electric vehicle and power grid applications.

Acknowledgments

This work was supported by the Korea Forest Research Institute FP 0400-2007-03 grant. This work was also supported by the leading industry of Sustainable Energy of the Chungcheong Leading Industry Office of the Korean Ministry of Knowledge Economy.

References

[1] W. Wei, J. Wang, L. Zhou, J. Yang, B. Schumann, Y. NuLi, Electrochem. Commun. 13 (2011) 399–402.
[2] M.H. Ryou, Y.M. Lee, J.K. Park, J.W. Choi, Adv. Mater. 23 (2011) 3066–3070.
[3] T. Kojima, T. Ishizu, T. Horiba, M. Yoshikawa, J. Power Sources 189 (2009) 859–863.
[4] J. Hassoun, S. Panero, P. Reale, B. Scrosati, Adv. Mater. 21 (2009) 4807–4810.
[5] H. Li, Z. Wang, L. Chen, X. Huang, Adv. Mater. 21 (2009) 4593–4607.
[6] C. Liu, F. Li, L. Ma, H. Cheng, Adv. Mater. 22 (2010) E28–E62.
[7] J.B. Goodenough, Y. Kim, Chem. Mater. 22 (2010) 587–603.
[8] G. Jeong, Y. Kim, H. Kim, Y. Kim, H. Sohn, Energy Environ. Sci. 4 (2011) 1986–2002.
[9] J.R. Selman, S. Al Hallaj, I. Uchida, Y. Hirano, J. Power Sources 97–98 (2001) 726–732.
[10] J. Cho, Y. Kim, B. Kim, J. Lee, B. Park, Angew. Chem. Int. Ed. 42 (2003) 1618–1621.
[11] J. Hassoun, P. Reale, B. Scrosati, J. Mater. Chem. 17 (2007) 3668–3677.
[12] M.R. Palacin, Chem. Soc. Rev. 38 (2009) 2565–2575.
[13] G. Venugopal, J. Moore, J. Howard, S. Pendalwar, J. Power Sources 77 (1999) 34–41.
[14] P. Arora, Z. Zhang, Chem. Rev. 104 (2004) 4419–4462.
[15] S.S. Zhang, J. Power Sources 164 (2007) 351–364.
[16] S. Augustin, V. Hennige, G. Hörpel, C. Hying, Desalination 146 (2002) 23–28.
[17] H.S. Jeong, J.H. Kim, S.Y. Lee, J. Mater. Chem. 20 (2010) 9180–9186.
[18] J.H. Cho, J.H. Park, J.H. Kim, S.Y. Lee, J. Mater. Chem. 21 (2011) 8192–8198.
[19] E.S. Choi, S.Y. Lee, J. Mater. Chem. 21 (2011) 14747–14754.
[20] T.H. Cho, M. Tanaka, H. Onishi, Y. Kondo, T. Nakamura, H. Yamazaki, S. Tanase, T. Sakai, J. Power Sources 181 (2008) 155–160.
[21] H.R. Jung, D.H. Ju, W.J. Lee, X. Zhang, R. Kotek, Electrochim. Acta 54 (2009) 3630–3637.
[22] C. Yang, Z. Jia, Z. Guan, L. Wang, J. Power Sources 189 (2009) 716–720.
[23] Z.J. Zhang, P. Ramadass, in: M. Yoshio, R.J. Brodd, A. Kozawa (Eds.), Lithium-ion Batteries: Science and Technologies, vol. 26, Springer, New York, 2009.
[24] Y.M. Lee, J.W. Kim, N.S. Choi, J.A. Lee, W.H. Seol, J.K. Park, J. Power Sources 139 (2005) 235–241.
[25] T.H. Cho, M. Tanaka, H. Ohnishi, Y. Kondo, M. Yoshikazu, T. Nakamura, T. Sakai, J. Power Sources 195 (2010) 4272–4277.
[26] S.J. Chun, E.S. Choi, E.H. Lee, J.H. Kim, S.Y. Lee, S.Y. Lee, J. Mater. Chem. 22 (2012) 16618–16626.
[27] I. Siró, D. Plackett, Cellulose 17 (2010) 459–494.
[28] S.J. Chun, S.Y. Lee, G.H. Doh, S. Lee, J.H. Kim, J. Ind. Eng. Chem. 17 (2011) 521–526.
[29] H. Yano, S. Nakahara, J. Mater. Sci. 39 (2004) 1635–1638.
[30] M. Henriksson, L.A. Berglund, P. Isaksson, T. Lindstrom, T. Nishino, Biomacromolecules 9 (2008) 1579–1585.
[31] M. Nogi, S. Iwamoto, A.N. Nakagaito, H. Yano, Adv. Mater. 21 (2009) 1595–1598.
[32] M. Paakko, J. Vapaavuori, R. Silvennoinen, H. Kosonen, M. Ankerfors, T. Lindstrom, L.A. Berglund, O. Ikkala, Soft Matter 4 (2008) 2492–2499.
[33] V. Nassehi, D.B. Das, I.M.T.A. Shigidi, R.J. Wakeman, Asia-Pac. J. Chem. Eng. 6 (2011) 850–862.
[34] P. Zhang, L.C. Yang, L. Li, Q.T. Qu, Y.P. Wu, M. Shimizu, J. Membr. Sci. 362 (2010) 113–118.
[35] P. Zhang, G.C. Li, H.P. Zhang, L.C. Yang, Y.P. Wu, Electrochem. Commun. 11 (2009) 161–164.
[36] N.H. Idris, M.M. Rahman, J. Wang, H. Liu, J. Power Sources 201 (2012) 294–300.
[37] A.A. Robertson, Tappi 53 (1970) 1331–1339.
[38] H.S. Jeong, S.Y. Lee, J. Power Sources 196 (2011) 6716–6722.
[39] J.R. Lee, J.H. Won, J.H. Kim, K.J. Kim, S.Y. Lee, J. Power Sources 216 (2012) 42–47.
[40] J.H. Park, J.H. Cho, W. Park, D.J. Ryoo, S.J. Yoon, J.H. Kim, S.Y. Lee, J. Power Sources 195 (2010) 8306–8310.
[41] H.S. Jeong, E.S. Choi, J.H. Kim, S.Y. Lee, Electrochim. Acta 56 (2011) 5201–5204.
[42] S.M. Oh, S.T. Myung, J.B. Park, B. Scrosati, K. Amine, Y.K. Sun, Angew. Chem. Int. Ed. 51 (2012) 1853–1856.
[43] W. Chang, J. Choi, J. Im, J.K. Lee, J. Power Sources 195 (2010) 320–326.
[44] J.H. Cho, J.H. Park, M.H. Lee, H.K. Song, S.Y. Lee, Energy Environ. Sci. 5 (2012) 7124–7131.